Electronic supplementary information

Room-temperature liquid metal-based self-healing anode for lithium-ion batteries with an ultra-long cycle life

Yingpeng Wu,* Lu Huang,* Xingkang Huang,* Xiaoru Guo, Dan Liu, Dong Zheng, Xuelin Zhang, Ren Ren, Deyang Qu, Junhong Chen†

Department of Mechanical Engineering, University of Wisconsin-Milwaukee, 3200 North Cramer Street, Milwaukee, WI, 53211, USA

*These authors contributed equally to this work.

Corresponding author email: jhchen@uwm.edu.

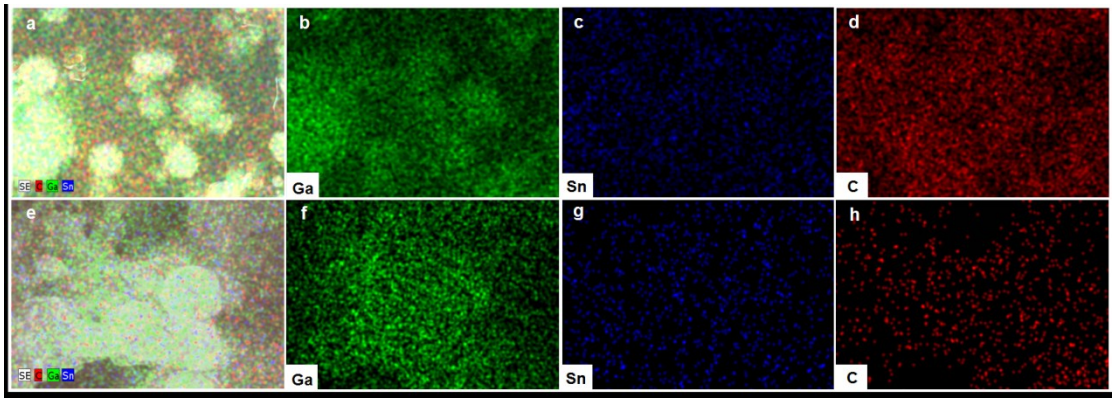

Fig. S1. (a) is the overlay image of SEM and the C, Ga, and Sn EDS images before cycling, (e) is that after cycling. EDS mapping images for C, Ga, and Sn before and after cycling, (b-d) C, Ga and Sn separately before cycling, (f-h) C, Ga, and Sn separately after cycling,

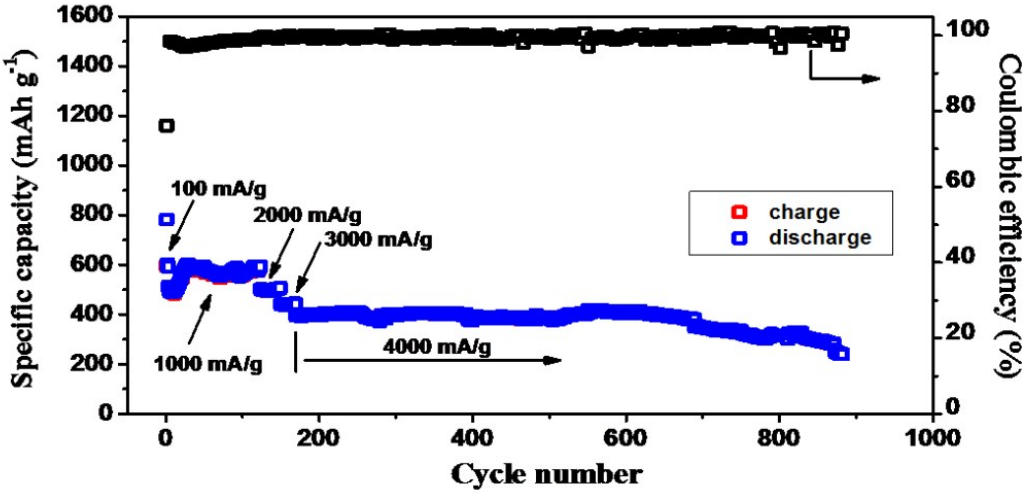

Fig. S2. Control experiment using the electrode without CNTs shows the cycle life is less than 900 cycles.

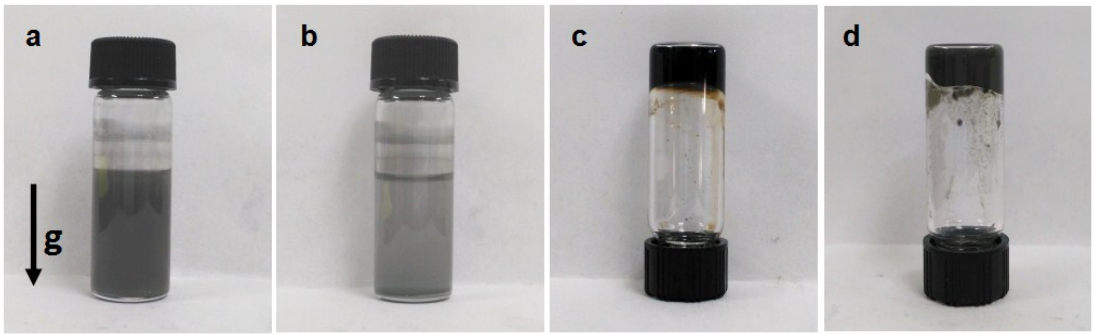

Fig. S3. (a) LMNPs suspension in ethanol after sonication. (b) Precipitated LMNPs after 24 h. (c) LMNPs mixed with GO gel after 24 h. (d) LMNPs mixed with CNTs and GO gel after 24 h. The arrow shows the gravity direction.

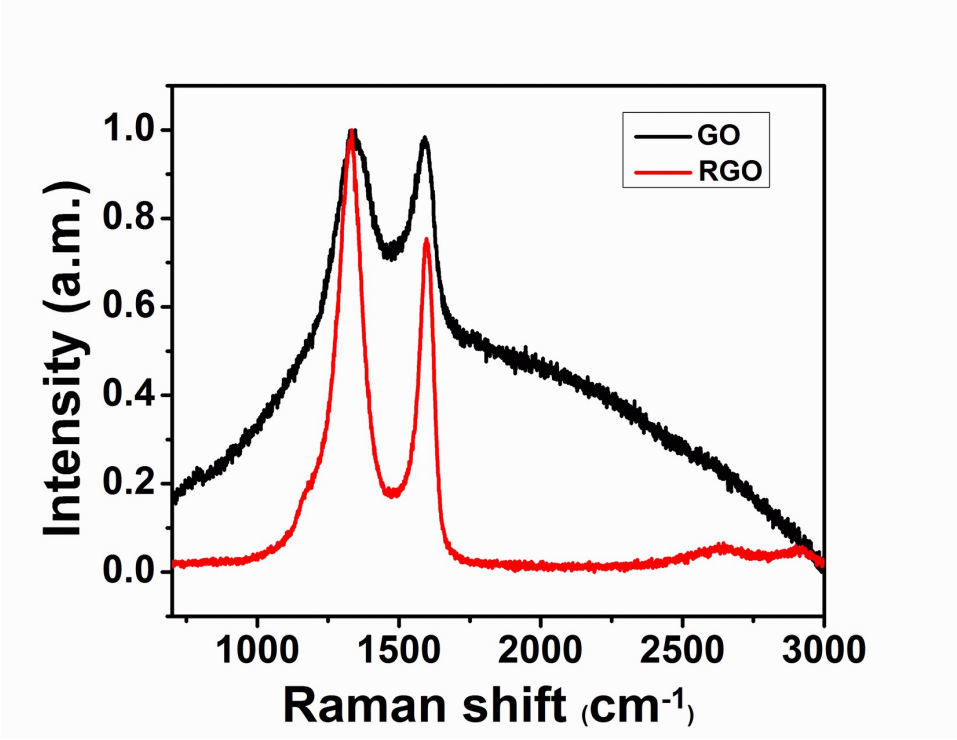

Fig. S4. Raman spectra of the GO and RGO after thermal treatment.

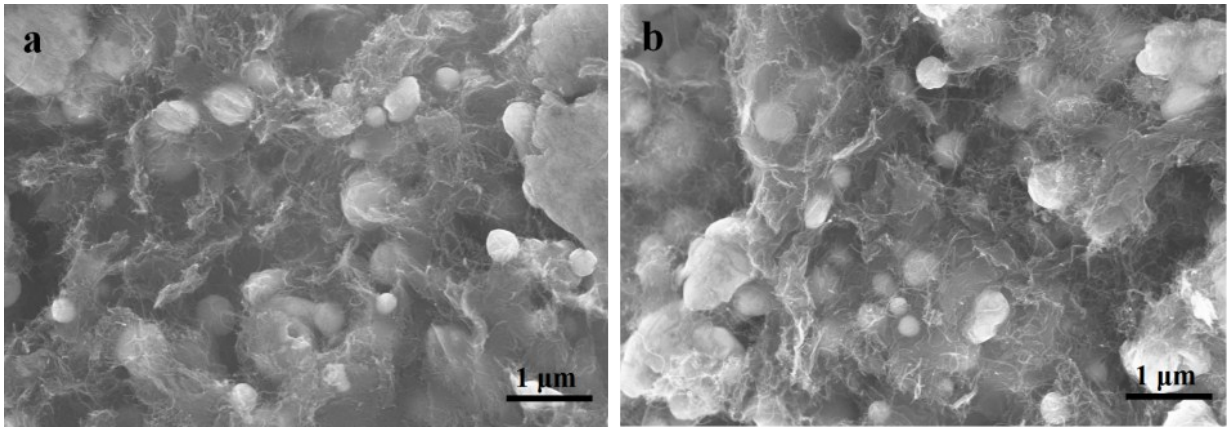

Fig. S5. Anode material before (a) and after (b) vibration test. There was no change in the size and shape of the LMNPs.

We did the dropping test of the battery. We dropped the battery at 2-m high onto a hard floor for over 50 times. The SEM images (Fig. S6) suggested there was no change of the morphology before (a) and after (b) dropping. And the electrochemical performance of the anode material was stable after dropping. The CV curves (Fig. S7) before and after dropping were overlapping, indicating high stability of the anode.

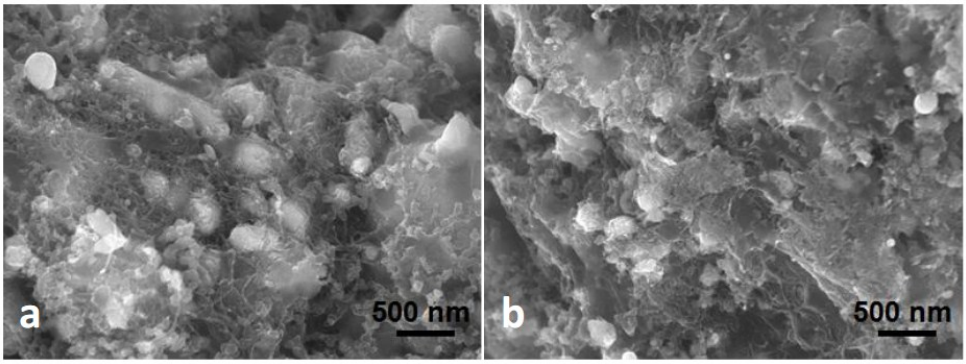

Fig. S6. SEM images of the anode material before (a) and after (b) the dropping.

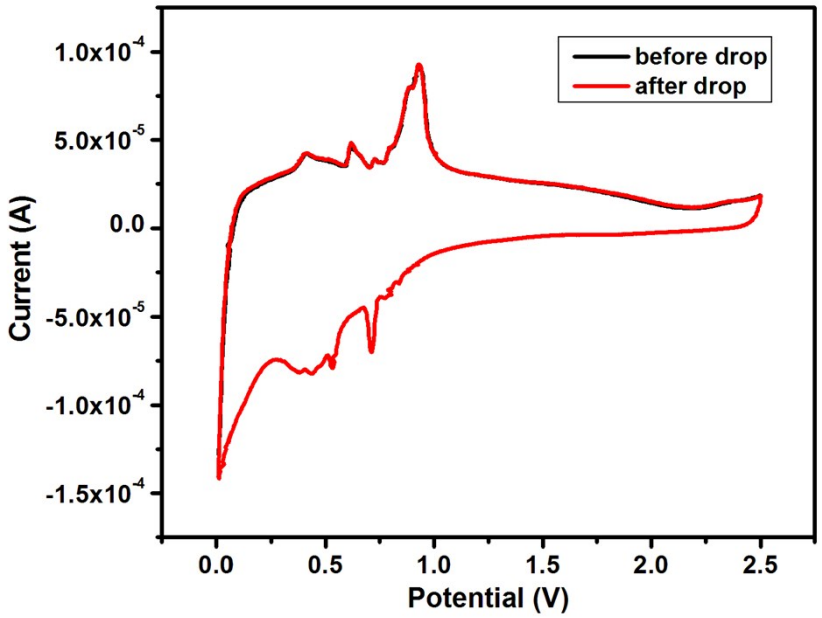

Fig. S7. The CV curves before and after dropping are overlapping, indicating a high stability of the anode.

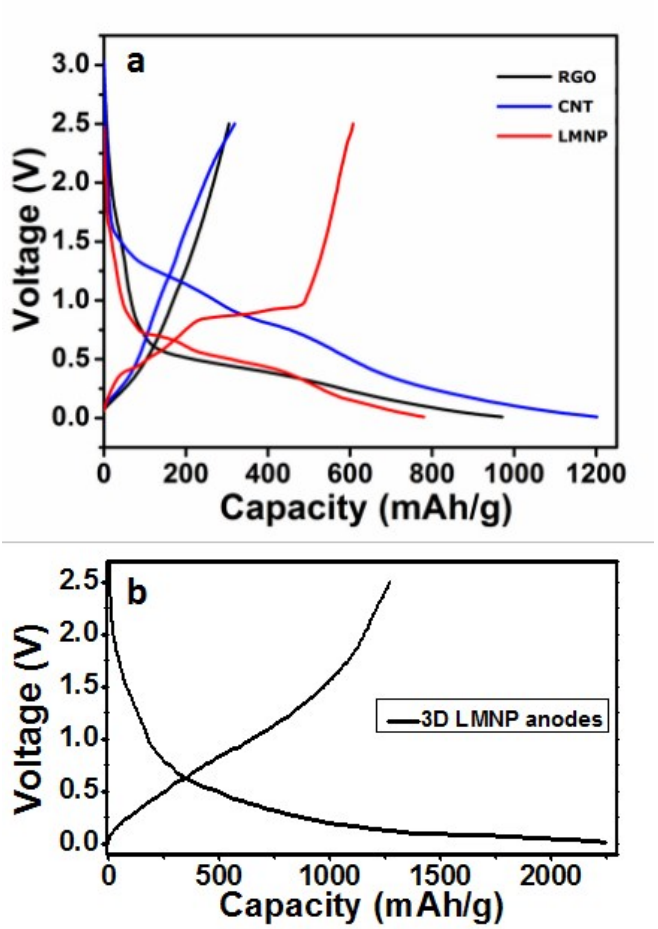

Fig. S8. (a) First charge/discharge performance of RGO, CNT, LMNP with a current of 200 mA/g. (b) First charge/discharge performance of 3D LMNP anode with a current of 200 mA/g.

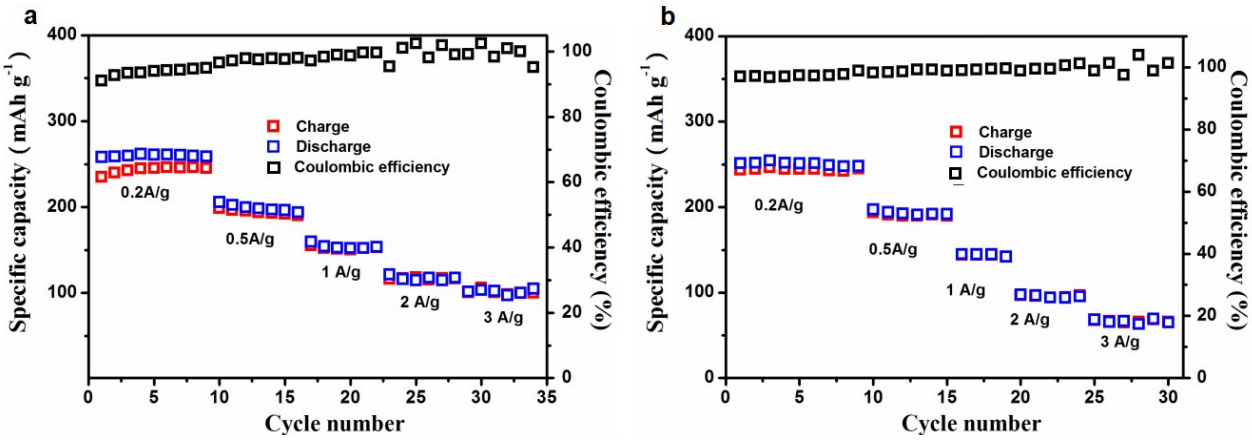

Fig. S9. The capacity and rate performance of CNTs (a) and RGO (b) under different

rates.

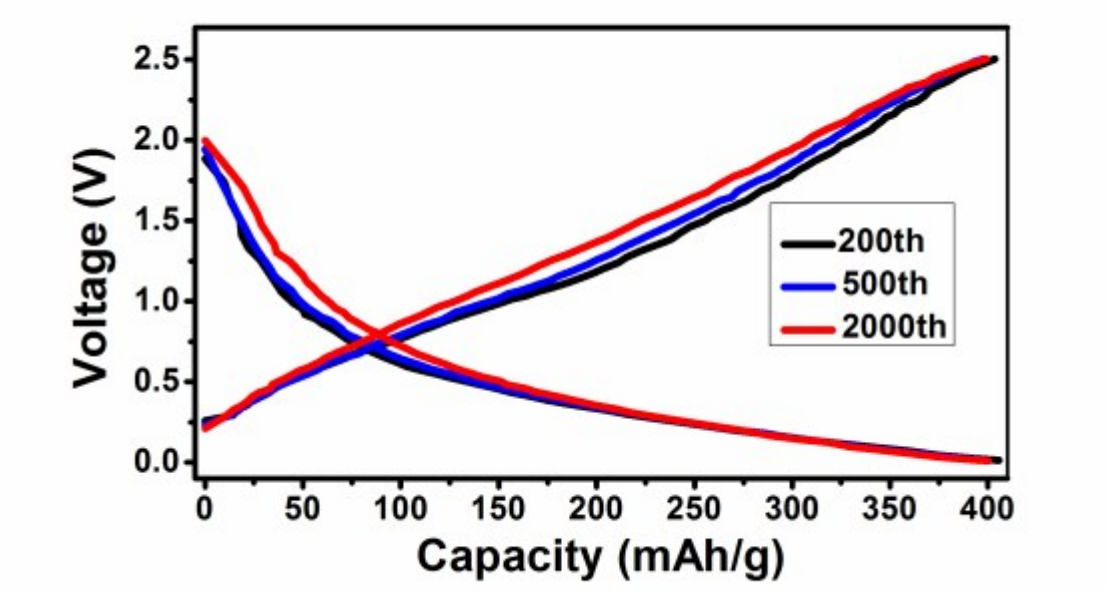

Fig. S10. Curves of different cycle numbers.

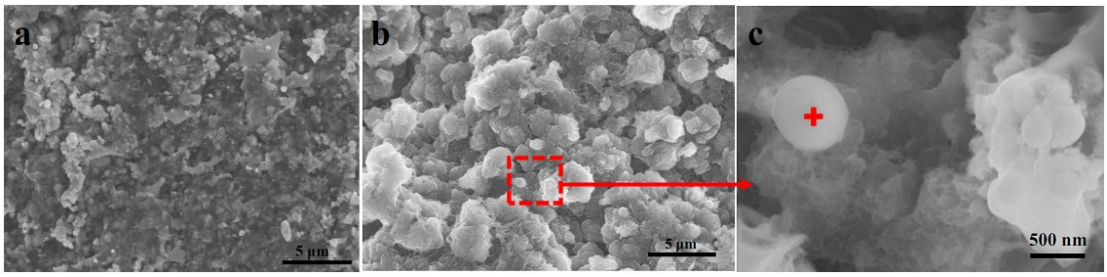

Fig. S11. (a) SEM image of the anode before cycling. (b) SEM image of the anode after more than 4,500 cycles. (c) the high-magnification image of the anode, showing the LMNPs.

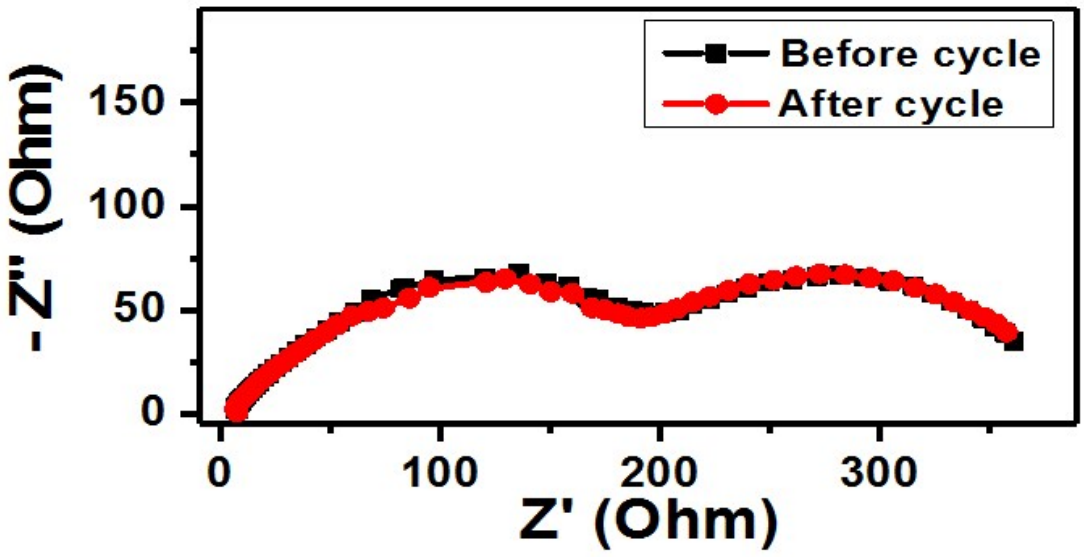

Fig. S12. Nyquist plots of the battery before and after cycling at the fully charged state.

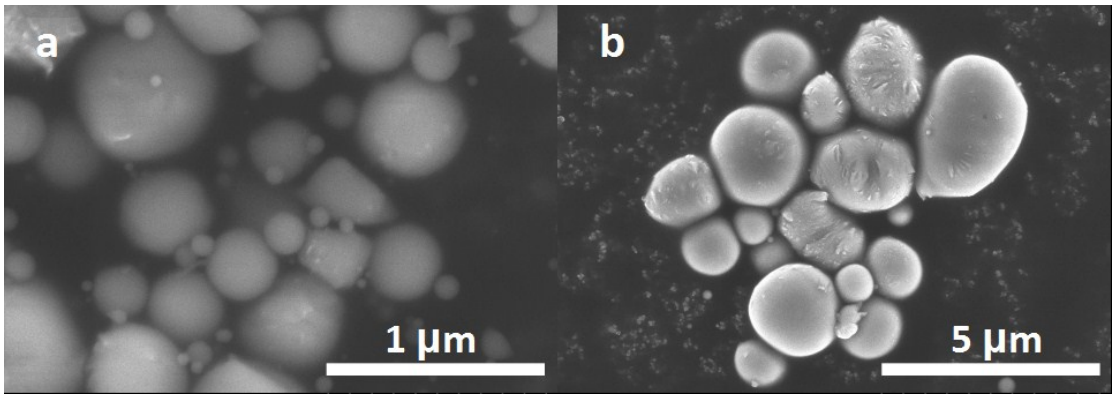

Fig. S13. LM particles with 1ATC9 (a) are much smaller than those without 1ATC9 (b) after sonication.

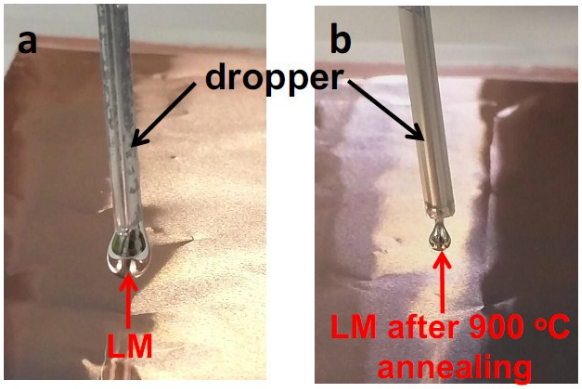

Fig. S14. The Ga-Sn alloy before (a) and after 900 °C annealing (b); both are in the liquid state.

Table S1| Comparison of anode performance between literature and the current work.

Anode	Cycle life	Capacity	Characteristic	Ref
Si	1,300	Fixed to 1,200 mAh/g at 1.2 A/g	Alginate binder	S1
Si	2,000	1,000 mAh/g at 4A/g	Silicon nanowire	S2
Sn	1,000	652 mAh/g at 2A/g	Graphene networks anchored Sn nanoparticles	S3
Sn	1,000	537 mAh/g at 3A/g	CNTs/carbon cubes networks anchored Sn nanoparticles	S4
Ga	30	~400 mAh/g, C/20 charging, C/5 discharging	Working at 40 °C	S5
Ga	100	400 mAh/g at 0.1 A/g	Working at 55 °C, Ga nanoparticles were embedded in carbon network	S6
Ge-Sn	1,700	890 mAh/g at 3 A/g	Ge-Sn composite	S7
Ge	1,200	1,080 mAh/g at 0.5 C	Crumpled N-doped carbon nanotubes encapsulated with Ge nanoparticles	S8
Sb	100	488 mAh/g at 0.1 A/g	Rod-like Sb-C composite	S9
Sn-M	20	227 mAh/g at 0.1 A/g (Sn-Fe)	Sn-M (M=Cu, Mg and Fe) intermetallic alloys	S10
Si with carbon	100	~800 mAh/g at 0.1 A/g	Self-healing polymer as binder	S11
Si	130	~2,000 mAh/g at 0.1 C	Self-healing polymer as binder	S12

This work	>4,000	780 mAh/g at 0.1 A/g, ~400 mAh/g at 4A/g after 4,000 cycles	Self-healing LM anode working at RT	

SI Video. In-situ micrograph during the charge/discharge process for the self-healing mechanism.

References for ESI

S1. I. Kovalenko, B. Zdyrko, A. Magasinski, B. Hertzberg, Z. Milicev, R. Burtovyy, I. Luzinov and G. Yushin, *Science*, 2011, **334**, 75.

S2. M. Ge, J. Rong, X. Fang and C. Zhou, *Nano Lett.*, 2012, **12**, 2318.

S3. J. Qin, C. He, N. Zhao, Z. Wang, C. Shi, E. Liu and J. Li, *ACS Nano*, 2014, **8**, 1728.

S4. X. K. Huang, S. M. Cui, J. B. Chang, P. B. Hallac, C. R. Fell, Y. T. Luo, B. Metz, J. W. Jiang, P. T. Hurley and J. H. Chen, *Angew. Chen. Int. Edit.*, 2015, **54**, 1490.

S5. R. D. Deshpande, J. C. Li, Y. T. Cheng and M. W. Verbrugge, *J. Electrochem. Soc.*, 2011, **158**, A845.

S6. K. T. Lee, Y. S. Jung, T. Kim, C. H. Kim, J. H. Kim, J. Y. Kwon and S. M. Oh, *Electrochem. Solid St.*, 2008, **11**, A21.

S7. N. Lin,J. Zhou,Y. Han,K. Zhang,Y. Zhu, and Y. Qian, *Chem. Commun*., 2015, **51**, 17156.

S8. K. Huo, L. Wang, C. Peng, X, Peng, Y. Li, Q. Li, Z. Jin and P. K. Chub, *J. Mater. Chem. A*, 2016, **4**, 7585

S9. L. Fan, J. Zhang, J. Cui, Y. Zhu, J. Liang, L. Wang and Y. Qian, *J. Mater. Chem. A*, 2015, **3**, 3276.

S10. S. Gao, A. Wu, X. Jin, F. Ye, X. Dong, J. Yu and Hao Huang, *J. Alloy. Compd*. 2017, **706**, 401.

S11. Y. M. Sun, J. Lopez, H. W. Lee, N. Liu, G. Y. Zheng, C. L. Wu, J. Sun, W. Liu, J. W. Chung, Z. N. Bao and Y. Cui, *Adv. Mater.*, 2016, **28**, 2455.

S12. C. Wang, H. Wu, Z. Chen, M. T. McDowell, Y. Cui and Z. A. Bao, *Nat. Chem.*, 2013, **5**, 1042.